

A Modified Hydro-Thermo-Diffusive Theory of Laminar Premixed Flames

SIAVASH H. SOHRAB

Robert McCormick School of Engineering and Applied Science
Department of Mechanical Engineering
Northwestern University, Evanston, Illinois 60208
UNITED STATES OF AMERICA

Abstract: - Scale-invariant forms of conservation equations in reactive fields are discussed. The modified forms of the conservation equations at eddy-dynamic, cluster-dynamic, and molecular-dynamic scales are then solved to describe the hydro-thermo-diffusive structure of premixed laminar flames. The predicted error-function type geometry of temperature profile as well as the flame thermal thickness are found to be in good agreement with the measurements reported in the literature. Also, the predicted propagation velocity of 42 cm/s for one-step combustion of stoichiometric methane-air premixed flame is in good agreement with the observations as well as numerical calculations based on multi-step kinetic models.

Key-Words: - Theory of laminar flames. Premixed combustion. Flame structure.

1 Introduction

The universality of turbulent phenomena from stochastic quantum fields to classical hydrodynamic fields resulted in recent introduction of a scale-invariant model of statistical mechanics and its application to the field of thermodynamics [4]. In the classical kinetic theory of gas by *Maxwell* and *Boltzmann*, particles are treated as point-mass singularities without any spatial extent. However, it is known that in reality molecules and atoms are not point-mass singularities but rather finite-size stable composite structures made of many smaller more elementary particles. Therefore, the fact that the classical approach of assuming point-mass entities has been successful in the description of molecular dynamics suggests that this same approach could be generalized to macroscopic scales.

Following such guidelines, a scale-invariant model of statistical mechanics for equilibrium fields of eddy-, cluster-, molecular-, atomic-dynamics corresponding to the scales $\beta = e, c, m, a$, schematically shown in Fig.1 was introduced [4] and applied to the derivation of the invariant forms of conservation equations [5] and the introduction of a modified hydro-thermo-diffusive theory of laminar flame [6]. In the present study, the invariant forms of the conservation equations are employed to further investigate the hydro-thermo-diffusive structure of laminar premixed flames. The predicted

temperature and velocity profiles as well as the laminar flame thickness are shown to be in accordance with the experimental measurements.

2 Scale-Invariant Forms of the Conservation Equations for Reactive Fields

Following the classical methods [1-3], the invariant definitions of the density ρ_β , and the velocity of *atom* \mathbf{u}_β , *element* \mathbf{v}_β , and *system* \mathbf{w}_β at the scale β are given as [5, 6]

$$\rho_\beta = n_\beta m_\beta = m_\beta \int f_\beta d\mathbf{u}_\beta \quad , \quad \mathbf{u}_\beta = \mathbf{v}_{\beta-1} \quad (1)$$

$$\mathbf{v}_\beta = \rho_\beta^{-1} m_\beta \int \mathbf{u}_\beta f_\beta d\mathbf{u}_\beta \quad , \quad \mathbf{w}_\beta = \mathbf{v}_{\beta+1} \quad (2)$$

Also, the invariant definitions of the peculiar and the diffusion velocities are given as [4]

$$\mathbf{V}'_\beta = \mathbf{u}_\beta - \mathbf{v}_\beta \quad , \quad \mathbf{V}_\beta = \mathbf{v}_\beta - \mathbf{w}_\beta = \mathbf{V}'_{\beta+1} \quad (3)$$

Next, following the classical methods [1-3], the scale-invariant forms of mass, thermal energy, and linear momentum conservation equations at scale β are given as [5, 6]

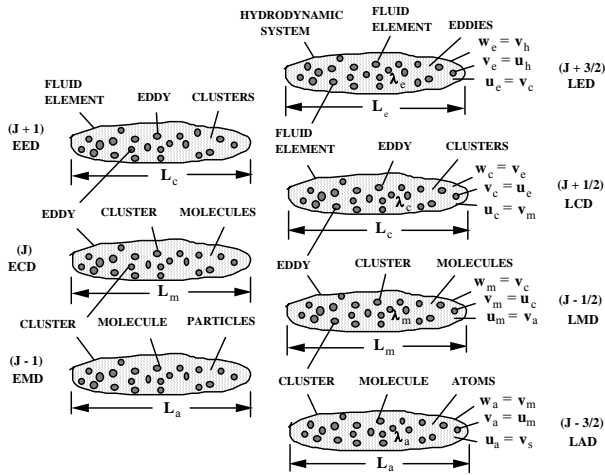


Fig.1 Hierarchy of statistical fields for equilibrium eddy-, cluster-, and molecular-dynamic scales and the associated laminar flow fields.

$$\frac{\partial \rho_\beta}{\partial t} + \nabla \cdot (\rho_\beta \mathbf{v}_\beta) = \Omega_\beta \quad (4)$$

$$\frac{\partial \varepsilon_\beta}{\partial t} + \nabla \cdot (\varepsilon_\beta \mathbf{v}_\beta) = 0 \quad (5)$$

$$\frac{\partial \mathbf{p}_\beta}{\partial t} + \nabla \cdot (\mathbf{p}_\beta \mathbf{v}_\beta) = -\nabla \cdot \mathbf{P}_\beta \quad (6)$$

involving the *volumetric density* of thermal energy $\varepsilon_\beta = \rho_\beta h_\beta$ and linear momentum $\mathbf{p}_\beta = \rho_\beta \mathbf{v}_\beta$. Also, Ω_β is the chemical reaction rate, h_β is the absolute enthalpy [5], and \mathbf{P}_β is the partial stress tensor [1]

$$\mathbf{P}_\beta = m_\beta \int (\mathbf{u}_\beta - \mathbf{v}_\beta)(\mathbf{u}_\beta - \mathbf{v}_\beta) f_\beta d\mathbf{u}_\beta \quad (7)$$

In the derivation of (6) we have used the definition of the peculiar velocity (3) along with the identity

$$\overline{\mathbf{V}'_{\beta i} \mathbf{V}'_{\beta j}} = \overline{(\mathbf{u}_{\beta i} - \mathbf{v}_{\beta i})(\mathbf{u}_{\beta j} - \mathbf{v}_{\beta j})} = \overline{\mathbf{u}_{\beta i} \mathbf{u}_{\beta j}} - \mathbf{v}_{\beta i} \mathbf{v}_{\beta j} \quad (8)$$

The summation of (6) over all the species results in the classical form of the equation of motion [1, 3]

$$\frac{\partial \rho \mathbf{w}}{\partial t} + \nabla \cdot (\rho \mathbf{w} \mathbf{w}) = -\nabla \cdot \mathbf{P} \quad (9)$$

where $\mathbf{w} = \mathbf{w}_\beta = \mathbf{v}_{\beta+1}$ is the mass-average velocity and the total or mixture stress tensor is [1, 3]

$$\mathbf{P} = \sum_\beta \mathbf{P}_\beta = \sum_\beta m_\beta \int (\mathbf{u}_\beta - \mathbf{v}_\beta)(\mathbf{u}_\beta - \mathbf{v}_\beta) f_\beta d\mathbf{u}_\beta \quad (10)$$

The local velocity \mathbf{v}_β in (4)-(6) is expressed in terms of the convective \mathbf{w}_β and the diffusive \mathbf{V}_β velocities [5]

$$\mathbf{v}_\beta = \mathbf{w}_\beta + \mathbf{V}_{\beta g}, \quad \mathbf{V}_{\beta g} = -D_\beta \nabla \ln(\rho_\beta) \quad (11a)$$

$$\mathbf{v}_\beta = \mathbf{w}_\beta + \mathbf{V}_{\beta t g}, \quad \mathbf{V}_{\beta t g} = -\alpha_\beta \nabla \ln(\varepsilon_\beta) \quad (11b)$$

$$\mathbf{v}_\beta = \mathbf{w}_\beta + \mathbf{V}_{\beta h g}, \quad \mathbf{V}_{\beta h g} = -v_\beta \nabla \ln(\mathbf{p}_\beta) \quad (11c)$$

where ($\mathbf{V}_{\beta g}$, $\mathbf{V}_{\beta t g}$, $\mathbf{V}_{\beta h g}$) are respectively the diffusive, the thermo-diffusive, the linear hydro-diffusive velocities.

Substitutions from (11a)-(11c) into (4)-(6), neglecting cross-diffusion terms and assuming constant transport coefficients with $Sc_\beta = Pr_\beta = 1$, result in [5, 6]

$$\frac{\partial \rho_\beta}{\partial t} + \mathbf{w}_\beta \cdot \nabla \rho_\beta - D_\beta \nabla^2 \rho_\beta = \Omega_\beta \quad (12)$$

$$\frac{\partial T_\beta}{\partial t} + \mathbf{w}_\beta \cdot \nabla T_\beta - \alpha_\beta \nabla^2 T_\beta = -h_\beta \Omega_\beta / (\rho_\beta c_{p\beta}) \quad (13)$$

$$\frac{\partial \mathbf{v}_\beta}{\partial t} + \mathbf{w}_\beta \cdot \nabla \mathbf{v}_\beta - v_\beta \nabla^2 \mathbf{v}_\beta = -\frac{\nabla p_\beta}{\rho_\beta} - \frac{\mathbf{v}_\beta \Omega_\beta}{\rho_\beta} \quad (14)$$

An important feature of the modified equation of motion (14) is that it is linear since it involves a convective velocity \mathbf{w}_β that is different from the local fluid velocity \mathbf{v}_β . Also, the last term of the modified form of the equation of motion (14) represents a source (sink) of momentum that is induced by exothermic (endothermic) chemical reaction.

3 Modified Theory of Laminar Premixed Flames

The theory of laminar flames is the most fundamental theory of combustion science and subject of many classical [7-16] as well as more recent [3, 17-23] investigations. The objective of the present study is to investigate the hydro-thermo-diffusive structure of a one-dimensional premixed flame. For planar flame propagation in an otherwise stationary combustible gas in the absence of any externally imposed convection the pressure gradients will be negligible and (12)-(14) reduce to [6]

$$\frac{\partial y}{\partial t'} = D \frac{\partial^2 y}{\partial x'^2} - \Lambda y e^{\beta(\theta-1)} \delta(x'_f) \quad (15)$$

$$\frac{\partial \theta}{\partial t'} = \alpha \frac{\partial^2 \theta}{\partial x'^2} + \Lambda y e^{\beta(\theta-1)} \delta(x'_f) \quad (16)$$

$$\frac{\partial v}{\partial t'} = \nu \frac{\partial^2 v}{\partial x'^2} + \nu \Lambda y e^{\beta(\theta-1)} \delta(x'_f) \quad (17)$$

The following dimensionless parameters have been defined

$$\theta = (T - T_u) / (T_b - T_u) , \quad y = Y_F / Y_{Fu} , \quad v = v' / v'_f$$

$$\rho_{Fu} = \rho Y_{Fu} , \quad \Lambda = (\nu_F W_F B / \rho) e^{-\beta/\chi} \quad (18)$$

The adiabatic flame temperature T_b , the *Zeldovich* number β , and the coefficient of thermal expansion χ are

$$T_b = T_u + QY_{Fu} / \nu_F W_F c_p$$

$$\beta = E(T_b - T_u) / RT_b^2 , \quad \chi = (T_b - T_u) / T_b \quad (19)$$

and one assumes that $\beta \gg 1$. Also, under the assumed unity *Prandtl*, *Schmidt*, and *Lewis* numbers, θ , y , and v fields will be similar under identical boundary conditions.

4 Hydro-Thermo-Diffusive Structure of Laminar Premixed Flames

Next, the hydro-thermo-diffusive structure of symmetric premixed flames is examined. The analysis of the complete structure of laminar flames requires considerations at three consecutive scales of LED, LCD, and LMD shown in Fig.1. These three spatial scales will respectively be associated with the far-field, the hydro-thermo-diffusive, and the reactive-diffusive coordinates that will be examined in the same sequence in the following.

4.1 The Far-Field Convective Coordinate

The description of flame at the LED scale corresponding to far-field convective coordinate is considered first. At this scale, the flame will appear as a mathematical surface of discontinuity. The field outside of the thin flame must be determined at the scale of LED with the relevant “atomic”, element, and system velocities (u_e , v_e , w_e) and the associated length scales

$$(l_e = 10^{-5}, \lambda_e = 10^{-3}, L_e = 10^{-1}) \text{ m} .$$

At the scale of LED the flame has no hydrodynamic structure and its velocity field in this

physical coordinate appears as a delta function schematically shown in Fig.2a. To arrive at the steady problem, one introduces a coordinate system moving with the flame

$$z' = x' + w'_{cz} t' \quad (20)$$

where $w'_{cz} = v'_f - v'_b / 2$ is constant only at the LED scale. However, the mean velocity w'_{cz} that is a constant at LED scale will turn out to have internal structure with spatial dependence at the next smaller scale of LCD [6] to be discussed in the following section. With the moving coordinate (20) the system (15)-(17) becomes

$$w'_{cz} \frac{dy}{dz'} = D \frac{d^2 y}{dz'^2} - \Lambda y e^{\beta(\theta-1)} \delta(z'_f) \quad (21)$$

$$w'_{cz} \frac{d\theta}{dz'} = \alpha \frac{d^2 \theta}{dz'^2} + \Lambda y e^{\beta(\theta-1)} \delta(z'_f) \quad (22)$$

$$w'_{cz} \frac{dv}{dz'} = \nu \frac{d^2 v}{dz'^2} + \nu \Lambda y e^{\beta(\theta-1)} \delta(z'_f) \quad (23)$$

The velocity jump v'_b across the flame is related to the laminar flame propagation velocity v'_f by the mass balance across the flame sheet $\rho_b(v'_f + v'_b) = \rho_u v'_f$. The temperature, mass fraction of the deficient component, and the velocity on either side of the flame sheet where the reaction is frozen $\Lambda = 0$ are obtained from the solution of (21)-(23) as

$$\theta = 1 - y = v = 0 \quad z' > 0 \quad (24)$$

$$\theta - 1 = y = v - v_b = 0 \quad z' < 0 \quad (25)$$

The velocity field on either side of the flame at LED scale is schematically shown in Fig.2.

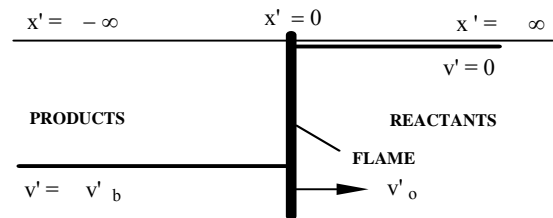


Fig.2 A propagating laminar flame viewed from far-field coordinate x' ($v'_o = v'_f$).

The allowance for coordinate dependence of w'_{cz} is an important distinction between the modified theory

and the classical theory that assumes a constant convective velocity $w'_{ze} = v'_f$. In the sequel it will become clear that the choice of variable convective velocity at LCD scale leads to the description of a flame front that propagates by diffusion, i.e. by Brownian motions, as opposed to one that moves as a rigid body.

4.2 The Hydro-Thermo-Diffusive Coordinate

To reveal the hydro-thermo-diffusive structure of the flame, one must move to the smaller scale of laminar cluster dynamics LCD with the characteristic velocities $(\mathbf{u}_c, \mathbf{v}_c, \mathbf{w}_c)$ and the associated length scales $(l_c = 10^{-7}, \lambda_c = 10^{-5}, L_c = 10^{-3})$ m. The subscript (c) refers to the laminar cluster-dynamic LCD scale with $\beta = c$ (Fig.1). The relevant kinematic viscosity for this scale is $\nu_c = l_c u_c / 3 = \lambda_m \nu_m / 3$ [5]. Also, for simplicity we assume that the Prandtl, Schmidt, and Lewis numbers are all equal to unity $\nu = \alpha = D$.

In a recent investigation on the modified theory of counterflow premixed flames [24] it was shown that free propagating laminar flames constitute a special case of symmetric counterflow laminar premixed flames schematically shown in Fig.3 that experience a strained flow field

$$w'_{ze} = -2\Gamma(z' - z'_f) \tag{26}$$

where $\Gamma = w'_{zo} / L$ is the stretch rate and L is the burner nozzle spacing (Fig.3). For the counterflow problem at LED scale an approximate solution of the modified equation of motion was shown to result in the stream function [24]

$$\Psi_c = -\frac{\xi_e^2}{2} \text{erf}(\zeta_c) \tag{27}$$

and the velocity components

$$v_{ze} = -\text{erf}(\zeta_c) \tag{28}$$

$$v_{re} = \frac{\xi_e}{\sqrt{\pi}} \exp(-\zeta_c^2) \tag{29}$$

where $\zeta_c = z' / \delta_c$ and $\delta_c = \sqrt{\nu_c / \Gamma}$. The axial and radial velocity profiles calculated from (28)-(29) are shown in Fig.3 and are in qualitative agreement with the experimental observations in Fig.8 of Yamaoka and Tsuji [25].

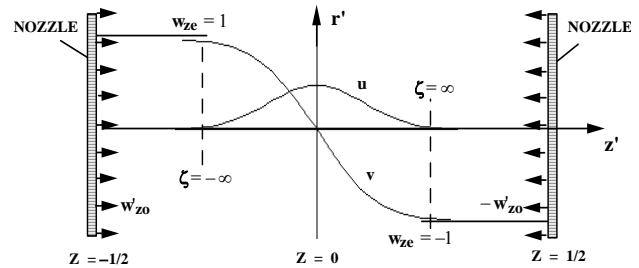


Fig.3 Calculated velocity profiles for axisymmetric finite-jet counterflow ($\mathbf{u} = \mathbf{v}_{re}, \mathbf{v} = \mathbf{v}_{ze}$) from (28)-(29).

The behavior of the counterflow premixed flame was found to depend on the relative magnitude of the jet axial velocity at infinity w'_{zo} versus the laminar flame propagation velocity v'_f such that one could identify four distinguishable burning regimes listed below [24]

- (a) When $w'_{zo} = 0$ two free-propagating flames propagate at the velocity $\mathbf{v}'_p = \mathbf{v}'_f$ towards $z' \rightarrow \pm\infty$ without experiencing any stretch.
- (b) When $w'_{zo} < -v'_f$ two flames propagate at the reduced velocity $\mathbf{v}'_p = \mathbf{v}'_f - w'_{zo}$ towards $z' \rightarrow \pm\infty$ without experiencing any stretch.
- (c) When $w'_{zo} = -(v'_f + \epsilon)$ and $\epsilon \ll 1$ two flames become stationary at $z'_f = \pm\delta_{fl}$ without experiencing any stretch.
- (d) When $w'_{zo} > -v'_f$ two flames are stationary at $z'_f < \pm\delta_{fl}$ and experience finite stretch.

The burning regime in case (c), when $w'_{zo} \approx -(v'_f + \epsilon)$ and the flame locates at the axial position corresponding to the edge of the boundary layer $L_e / 2 = \delta_{He} \approx 2\delta_c$ (the dashed lines in Fig.3) without experiencing any stretch, is identical to that of free-propagating laminar flame. The value of the stretch rate at LED scale for the case (c) will be $\Gamma_{ef} = w'_{zo} / L_e = v'_f / 4\delta_c$.

For analysis of the hydrodynamic structure of a free-propagating flame at LCD scale, it is first noted that the only actual non-random gas velocity is that of combustion products that move at v'_b with respect to stagnant reactants (Fig.2). The propagation velocity v'_f is the velocity of the thermal wave that passes through the reactants by diffusion. One can view the hydrodynamic flame structure as a “counterflow” (Fig.3) with the total change in the gas velocity v'_b across the flame thermal thickness of $L_c = 2\delta_{He} \approx 4\delta_c$ from $-v'_b / 2$

to $v'_b / 2$. Therefore, the effective stretch within the flame structure will be $\Gamma_f = (v'_b / 2) / 4\delta_c = v'_b / 8\delta_c$. Also, for LCD scale the characteristic diffusion length within the flame structure is defined as $\delta_c = \ell_T = \alpha / v'_f$. In the previous study [24] it was shown that the appropriate scaling factor between LED and LCD fields is $\delta_c = 4\delta_c$. Similar to $\delta_c = \sqrt{v_c / \Gamma}$ for the strained velocity field (26) at LED scale, δ_c at LCD scale could also be expressed as

$$\delta_c = \delta_{cf} = \sqrt{v / \Gamma_{cf}} = \ell_T \tag{30}$$

where $\Gamma_{cf} = v'_f / \ell_T$ such that $\Gamma_{cf} = 16\Gamma_{ef}$.

In view of the above considerations, parallel to (26) one expresses the convective velocity within the hydrodynamic structure of a free-propagating laminar flame at LCD scale as

$$w'_{cz} = -2\Gamma_f z' \tag{31}$$

with the self-induced flame stretch defined as [24]

$$\Gamma_f = \frac{v'_b}{8\delta_c} = \frac{v'_b}{8\ell_T} \tag{32}$$

For the analysis of hydro-thermo-diffusive flame structure one introduces the stretched coordinate

$$\eta = \frac{z' \sqrt{v_b}}{2\sqrt{2}\ell_T} \tag{33}$$

where $v_b = v'_b / v'_f$. By substitutions from (31)-(33) into (21)-(23) and noting the assumptions $v = \alpha = D$ one obtains

$$2\eta \frac{dy}{d\eta} + \frac{d^2y}{d\eta^2} = \frac{8\Lambda\alpha}{v_b v_f'^2} y e^{\beta(\theta-1)} \delta(\eta_r) \tag{34}$$

$$2\eta \frac{d\theta}{d\eta} + \frac{d^2\theta}{d\eta^2} = -\frac{8\Lambda\alpha}{v_b v_f'^2} y e^{\beta(\theta-1)} \delta(\eta_r) \tag{35}$$

$$2\eta \frac{dv_{zc}}{d\eta} + \frac{d^2v_{zc}}{d\eta^2} = -v_{zc} \frac{8\Lambda\alpha}{v_b v_f'^2} y e^{\beta(\theta-1)} \delta(\eta_r) \tag{36}$$

that are subject to the boundary conditions

$$\eta \rightarrow \infty \quad \theta = y - 1 = v_{zc} = 0 \tag{37a}$$

$$\eta \rightarrow -\infty \quad \theta - 1 = y = v_{zc} - v_b = 0 \tag{37b}$$

It is important to note that the delta functions associated with the reaction terms in (34)-(36) have

now been moved from the position of the flame z'_f in (21)-(23) of the far field coordinate (Fig.2) to the position of the reaction zone η_r of the thermo-diffusive coordinate η (Fig.4a).

The solutions of the system (34)-(37) outside of the thin reaction zone where because of $\beta \gg 1$ in (19) chemical reactions are frozen $\Lambda = 0$ are

$$\theta = 1 - y = \frac{1}{2} \text{erfc}(\eta) \tag{38}$$

$$v_{zc} = \frac{v_b}{2} \text{erfc}(\eta) \tag{39}$$

The predicted temperature profile (38) has error-function type geometry as schematically shown in Fig.4a.

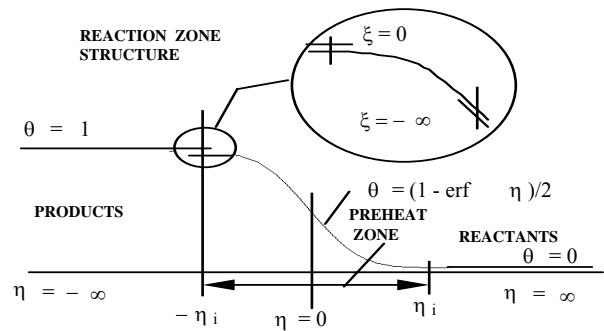


Fig.4a Flame structure according to the modified theory of laminar flames.

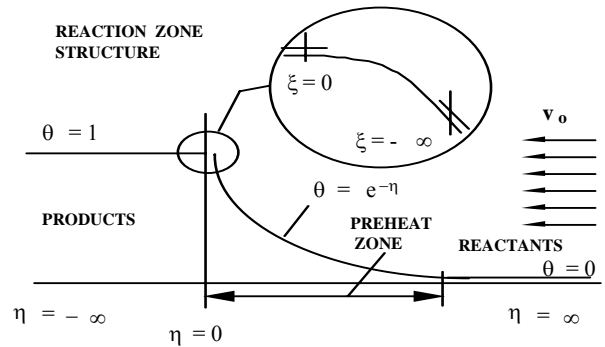


Fig.4b Flame structure according to the classical theory of laminar flames.

To facilitate the comparisons, the temperature profile according to the classical theory of laminar flame is schematically shown in Fig.4b. The predicted error-function type geometry of temperature profile of free-propagating laminar flames (38) is in accordance with the measured temperature profiles reported in the literature [26-29] that are all similar to the schematic diagram shown in Fig.81 of *Lewis and von Elbe* [30].

Attention is next focused on the sign of the curvature of the temperature profile near the reaction

zone in Fig.4a and the fact that the temperature in the reaction zone matches that in the preheat zone from above. By comparison, the sign of the curvature of temperature profile near the reaction zone according to the classical theory of laminar flames schematically shown in Fig.4b is opposite to that in Fig.4a. As a result, the temperature within the reaction zone must be matched to that in the preheat zone from below. However, this violates the fact that temperature in the reaction zone must be higher than that in the preheat zone.

The schematic diagram of the calculated hydrodynamic flame structure is shown in Fig.5.

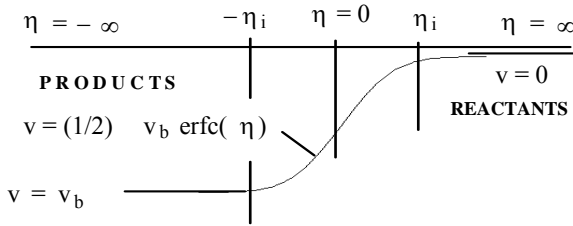


Fig.5 Hydrodynamic structure of a stationary laminar flame viewed from thermo-diffusive coordinate η ($v = v_{zc}$).

The asymmetry in the gas motion towards combustion products induced by expansion seen in Fig.5 is because of the fact that the upstream cold reactants are much heavier than the downstream hot products $\rho_u / \rho_b > 1$. As a result, the reactant side of the flame acts as an anchor against which the expanding gas can exert a force. Of course, the constant velocity of combustion products v'_b is achieved incrementally as the gas is accelerated within the flame hydrodynamic structure (Fig.5).

4.3 The Reactive-Diffusive Coordinate

The analysis of the much thinner reaction zone that is embedded within the hydro-thermo-diffusive zone follows the classical methods [3, 17-22] as described in an earlier study [6]. Since the reaction zone thickness is about δ_f/β and the *Zeldovich* number defined in (19) is large $\beta \gg 1$, under the present model the analysis of the reaction zone requires moving to the next smaller scale of laminar molecular-dynamics LMD (Figs.1, 4a) with the characteristic velocities ($\mathbf{u}_m, \mathbf{v}_m, \mathbf{w}_m$) and the associated length scales ($l_m = 10^{-9}$, $\lambda_m = 10^{-7}$, $L_m = 10^{-5}$) m. For the analysis of the thin reaction zone the stretched coordinate

$$\xi = \beta(\eta_i - \eta) \quad (40)$$

and the temperature and concentration expansions

$$\theta = 1 + \Theta_1/\beta + \dots, \quad y = 0 + Y_1/\beta + \dots \quad (41)$$

are introduced into (34)-(35) to obtain to the first order in $\epsilon = 1/\beta \ll 1$

$$\frac{d^2 Y_1}{d\xi^2} = \frac{8\Lambda\alpha}{v_b v_f'^2 \beta^2} Y_1 e^{\Theta_1} \quad (42)$$

$$\frac{d^2 \Theta_1}{d\xi^2} = -\frac{8\Lambda\alpha}{v_b v_f'^2 \beta^2} Y_1 e^{\Theta_1} \quad (43)$$

From the coupling of (42)-(43) and the boundary conditions at $\xi \rightarrow \pm\infty$ one obtains $\Theta_1 + Y_1 = 0$ such that (43) can be expressed as

$$\frac{d}{d\Theta_1} \left(\frac{d\Theta_1}{d\xi} \right)^2 = \frac{16\Lambda\alpha}{v_b v_f'^2 \beta^2} \Theta_1 e^{\Theta_1} \quad (44)$$

The first integral of the above equation and matching of the slopes of the temperature profiles on either side of the reaction zone with the outer solution in (25) and (38) result in

$$\exp(-2\eta_i^2) = \frac{16\pi v_F W_F B \alpha}{\rho v_b v_f'^2 \beta^2} \Theta_1 e^{\Theta_1} \quad (45)$$

that relates the reaction zone position η_i and hence the ignition temperature θ_i , to the flame propagation velocity v'_f . Because of the introduction of flame stretch (32) the result (45) differs from that reported in the earlier study [6] by a factor of 2.

The parameter B in (45) is related to the actual pre-exponential factor B' by the law of mass action [3] under *Arrhenius* kinetics as

$$B = B' \rho_F \rho_O / (W_F W_O) \quad (46)$$

Also, the mass balance across the flame front $\rho_b(v'_f + v'_b) = \rho_u v'_f$ leads to

$$v'_b = v'_f(\rho_u - \rho_b) / \rho_b \quad (47)$$

By substitutions from (46)-(47) into (45), one obtains the analytic expression

$$v_f'^2 = \frac{16\pi v_F \rho_b \rho_O \alpha B'}{(\rho_u - \rho_b) W_O \beta^2} e^{-\beta/\lambda} \exp(2\eta_i^2) \quad (48)$$

for the calculation of laminar flame propagation velocity.

For single-step overall combustion of stoichiometric premixed methane-air flame at the flame temperature of 2100 K the relevant physico-chemical properties are $v_F = 1$, $\rho_F = \rho_u$, $\rho_O = 1.38$

kg/m³, $W_o = 32$, $\alpha \approx 2.25 \times 10^{-4}$ m²/s (thermal diffusivity of air at the average temperature of 1200 K), $E \approx 46$ kcal/mole, $B' \approx 4.33 \times 10^7$ m³/kmol-s [31], $\chi \approx 0.86$, $\beta \approx 10$, and the ignition temperature of $\theta_i \approx 0.98$ that by (38) gives the reaction zone position $\eta_i \approx 1.48$. Also, from the temperatures of reactants 300 K and combustion products 2100 K and the ideal gas law under constant pressure, one obtains the density ratio $\rho_u / \rho_b = 7$. With these realistic values of the physico-chemical properties, the value of flame propagation velocity calculated from (48) is $v'_f \approx 42$ cm/s in close agreement with the experimentally observed values [26, 32-36]. Although this level of agreement between the theory and experiments is considered to be encouraging, it should be viewed with caution because of the well-known uncertainties in the ignition temperature and the overall chemical-kinetic parameters (E , B') [31]. The value of about $v'_f = 42$ cm/s has also been obtained in a number of numerical investigations using complex multi-step kinetic models [37-39].

5. Comparisons with Measured Flame Thermal Thickness and Temperature Profiles

As was described in the previous section, for the case (c) the structure of free-propagating laminar premixed flame is identical to that of the stationary symmetric counterflow premixed flame. The temperature profiles of lean methane-air premixed flames measured at constant equivalence ratio of $\phi = 0.8$ in the stagnation-point flow against the flat surface of a quartz plate from an earlier investigation [40] for the nozzle velocities $w'_{zo} = (30, 50, 70)$ cm/s and nozzle rim to plate spacing $L/2 = 1.26$ cm are shown in Fig.6.

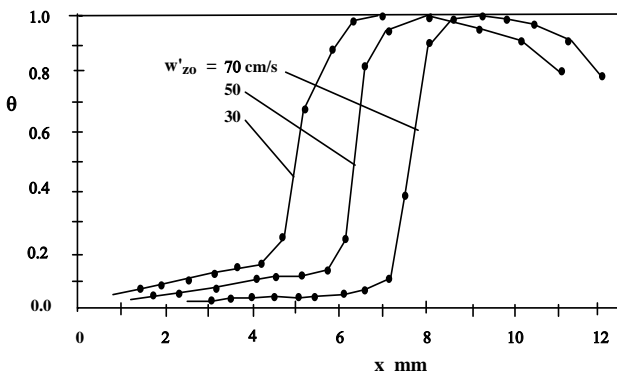


Fig.6 Measured temperature profiles for methane-air premixed flames in stagnation-point flow with $\phi = 0.8$, $L/2 = 1.26$ cm, $x = z'$, and $w'_{zo} = (30, 50, 70)$ cm/s [40].

The measured flame temperature will be somewhat reduced due to downstream heat loss to the quartz plate. However, even with symmetric counterflow premixed flames, because of the radiant heat loss one cannot achieve truly adiabatic premixed flames [41, 42]. The data in Fig.6 are similar to the temperature profiles reported in an earlier study [43]. For velocities below 70 cm/s, the gas leaving the burner is above ambient temperature of 300 K, thus complicating the evaluation of the flame thickness. Since thermocouple wire tends to slightly “drag” the flame along with it, the measured flame thicknesses are expected to be slightly larger than the actual ones. From the temperature profiles in Fig.6 the flame thermal thicknesses of about (3.0, 2.5, 2.0) mm are estimated for the nozzle velocities $w'_{zo} = (30, 50, 70)$ cm/s.

The predicted temperature profile of symmetric counterflow premixed flame [24]

$$\theta = \frac{1}{2} \operatorname{erfc}(\zeta - \zeta_f) \tag{49}$$

also involves error function similar to (38). According to the solution (49) upstream and downstream edges of the flame to an accuracy of 0.995 will be respectively at $(\zeta_+ - \zeta_f) = 2$ and $(\zeta_- - \zeta_f) = -2$ such that the predicted thickness of counterflow premixed flame ℓ_f becomes [24]

$$\ell_f = \sqrt{v/\Gamma} \tag{50}$$

indicating that ℓ_f decreases with Γ in accordance with the experimental observations shown in Fig.6.

For the measured flame temperature of 1500 K [40] and the average temperature of 900 K the thermal diffusivity of air is about $\varepsilon \approx v \approx 1.4$ cm²/s. Also, since the experiments [40] involve stagnation-point flow rather than counter flow, with an estimated boundary layer thickness of 2.5 mm [24] the burner distance becomes $L/2 = 1.26 - 2.5 \approx 1$ cm that gives the nozzle separation distance of $L = 2$ cm. Hence, the nozzle velocities $w'_{zo} = (30, 50, 70)$ cm/s will give by (27) the stretch rates $\Gamma = (15, 25, 35)$ s⁻¹ such that the predicted flame thermal thicknesses calculated from (50) become $\ell_f = (3.0, 2.4, 2.0)$ mm in good agreement with the measured values (3.0, 2.5, 2.0) mm estimated from Fig.6.

According to (38) the positions ($\eta_+ \approx 2, \eta_- \approx -2$) respectively correspond to the

upstream and the downstream edges of the flame thermal thickness to an accuracy of 0.995 leading to the predicted flame thermal thickness $\eta_+ - \eta_- = 4$ that by (33) results in

$$\delta_f \approx 8\sqrt{2}(\alpha / \sqrt{v'_f v'_b}) \quad (51)$$

From the mass balance across the flame $\rho_b(v'_f + v'_b) = \rho_u v'_f$ and the ideal gas law under the assumption of constant pressure one obtains

$$v'_b = v'_f(\rho_u / \rho_b - 1) = v'_f(T_b / T_u - 1) \quad (52)$$

Therefore, for the typical average temperature ratio of $T_b / T_u = 5$, one obtains from (52) the typical velocity ratio $v'_b = 4v'_f$ such that (51) becomes

$$\delta_f = \frac{8\sqrt{2}}{\sqrt{(T_b / T_u - 1)}} \frac{\alpha}{v'_f} = 4\sqrt{2}\ell_T \quad (53)$$

that is a factor of $2\sqrt{2}$ larger than the result reported by *Turns* [44]. The result (49) satisfies the required spatio-temporal invariance of a flame front propagating by diffusion $x' = 4\sqrt{2\alpha t'}$ such that $x' = \delta_f$ when $t' = \alpha / v'^2_f$. One notes that with $v'_b \approx 4v'_f$ the self-induced flame stretch (32) becomes $\Gamma_f = v'_f / 2\ell_T$.

For the methane-air premixed flame at $\phi = 0.8$ the flame propagation velocity is about 30 cm/s [26, 35, 36]. Therefore, the temperature profile for $w'_{z0} = 30$ cm/s shown in Fig.6 is expected to be very close to the temperature profile of a free-propagating laminar premixed flame in the absence of stretch effects that corresponds to the case (c) identified in Sec.4 above. At $\phi = 0.8$, at the mean adiabatic temperature of 1000 K, with $\alpha = 1.6$ cm²/s and $v'_f = 30$ cm/s the predicted laminar flame thickness from (53) is $\delta_f \approx 3.0$ mm in agreement with the data of Fig.6. In the study of *Eng et al* [29] for lean methane-air premixed flame at $\phi = 0.7$ stabilized on a flat burner, the flame thermal thickness of about 3.0 mm was measured at the flame temperature of about 1600 K. Now, for the average temperature of 950 K, the thermal diffusivity of air is about $\alpha = 1.55$ cm²/s such that for the flame speed of $v'_f = 23$ cm/s at $\phi = 0.7$ [26, 35, 36] the predicted flame thermal thickness becomes $\delta_f = 3.8$ mm. Since $\delta_f = 3.0$ mm at $\phi = 0.8$ as discussed above, one expects that $\delta_f > 3.0$ mm for $\phi = 0.7$ as predicted. Therefore, the

discrepancy could be caused by the fact that flat-plate flame [29] does not behave like a true free-propagating laminar flame. In comparison to the result (53), the predicted flame thermal thickness according to the classical theory of laminar flames is

$$\delta_f \approx \ell_T = \alpha / v'_f \quad (54)$$

that in general will deviate from the experimental measurements by a factor of about $4\sqrt{2}$.

6 Concluding Remarks

Scale-invariant forms of the conservation equations for energy, species mass fractions, and momentum in chemically reactive fields were employed to present a modified hydro-thermo-diffusive theory of laminar premixed flames. The predicted flame temperature profile and the flame thermal thickness were shown to be in accordance with the experimental measurements for lean methane-air premixed flames reported in an earlier investigation and those available in the literature.

Acknowledgements:

This research was in part supported by NASA micro-gravity combustion science program under grant NAG3-1863.

References:

- [1] de Groot, R. S., and Mazur, P., *Nonequilibrium Thermodynamics*, North-Holland, 1962.
- [2] Schlichting, H., *Boundary-Layer Theory*, McGraw Hill, New York, 1968.
- [3] Williams, F. A., *Combustion Theory*, 2nd Ed., Addison-Wesley, New York, 1985.
- [4] Sohrab, S. H., *Rev. Gén. Therm.* **38**, 845 (1999).
- [5] Sohrab, S. H., Transport phenomena and conservation equations for multi-component chemically reactive ideal gas mixtures. *Proceeding of the 31st ASME National Heat Transfer Conference*, HTD-Vol. **328**, 37-60 (1996).
- [6] Sohrab, S. H., *WSEAS Transactions on Mathematics*, Issue 4, Vol.3, 755 (2004).
- [7] Mallard, E., and le Chatelier, H. L., *Ann. de Mines* **4**:379 (1883).
- [8] Mikhel'son, V. A., Thesis, University of Moscow, 1889, see *Collected Works*, vol.1, Moscow: Novyi Agronom Press, 1930.
- [9] Taffanel, M., *Compt. Rend. Acad. Sci., Paris* **157**:714; **158**:42 (1913).
- [10] Jouguet, E., *Compt. Rend. Acad. Sci., Paris* **156**, 872 (1913); **179**, 274 (1924).
- [11] Nusselt, W., *Z. des Vereins Deutscher Ingenieure* **59**:872 (1915).
- [12] Daniell, P. J., *Proc. Roy. Soc. London* **126** A:393 (1930).
- [13] Lewis, B., and von Elbe, G., *J. Chem. Phys.* **2**:537 (1934).

- [14] Jost, W., and Müffling, L. V., *Z. Physik. Chem. A* **181**:208 (1937).
- [15] Kolmogoroff, A., Petrovsky, I., and Piscounoff, N., *Bulletin de l'université d'état à Moscou*, Série internationale, section A, Vol. 1 (1937), English translation in *Dynamics of Curved Fronts*, P. Pelcé (ed.), Academic Press, New York, 1988.
- [16] Zeldovich, J. B. and Frank-Kamenetski, D. A., *Acta Physicochimica U.R.S.S.*, vol. IX, No.2 (1938). English translation in *Dynamics of Curved Fronts*, P. Pelcé (ed.), Academic Press, New York, 1988.
- [17] Bush, W. B., and Fendell, F. E., *Combust. Sci. Technol.* **1**:421 (1970).
- [18] Williams, F. A., *Ann. Rev. Fluid Mech.* **3**:171 (1971).
- [19] Liñán, A., *Acta Astronautica* **1**, 1007 (1974).
- [20] Joulin, G., and Clavin, P., *Combust. Flame* **35**, 139 (1979).
- [21] Clavin, P., *Prog. Energy Combust. Sci.* **11**, 1 (1985).
- [22] Buckmaster, J. D., and Ludford, G. S. S., *Theory of Laminar Flames*, Cambridge University Press, Cambridge, 1982.
- [23] Warnatz, J., Maas, U., and Dibble, R. W., *Combustion*, Springer, New York, 1996.
- [24] Sohrab, S. H., *IASME Transactions*. Issue **7**, Vol.2, 1097 (2005); *IASME Transactions*, to appear.
- [25] Yamaoka, I., and Tsuji, H., *Proc. Combust. Inst.* **17**, p. 843 (1978).
- [26] Andrews, G. E., and Bradley, D., *Combust. Flame* **19**, 275 (1972); **20**, 77 (1973).
- [27] Fristrom, R. M., Grunfelder, C., and Favin, J., *J. Phys. Chem.* **64**, 1386 (1960).
- [28] Ferguson, R. C., and Keck, C. J., *Combust. Flame* **34**, 85 (1979).
- [29] Eng, J. A., Zhu, D. L., and Law, C. K., *Combust. Flame* **100**, 645 (1995).
- [30] Lewis, B., and von Elbe, G., *Combustion Flame and Explosion of Gases*, Academic Press, New York (1987).
- [31] Sohrab, S. H., Ye, Z. Y., Law, C. K., *Combust. Sci. Technol.* **45**, 27 (1986).
- [32] Günther, R., and Janisch, G., *Combust. Flame* **19**, 49 (1972).
- [33] Lindow, R., *Brennstoff Wärme Kraft* **20**, 8 (1968).
- [34] Reed, S. B., Mineur, J., and McNaughton, J. P., *J. Inst. Fuel* **44**, 149 (1971).
- [35] Yamaoka, I., and Tsuji, H., *Proc. Combust. Inst.* **20**, p. 1883 (1984).
- [36] Wu, C. K., and Law, C. K., *Proc. Combust. Inst.* **20**, p. 1941 (1978).
- [37] Smoot, D. L., Hecker, W. C., and Williams, G. A., *Combust. Flame* **26**, 323 (1976).
- [38] Tsatsaronis, G., *Combust. Flame* **33**, 217 (1978).
- [39] Chen, C. L., and Sohrab, S. H., *Combust. Flame* **101**, 360 (1995).
- [40] Kurz, O., and Sohrab, S. H., *First Joint Western-Central-Eastern States Section Meeting*, The Combustion Institute, March 14-17, 1999, George Washington University, Washington DC.
- [41] Liu, G. E., Ye, Z. Y., and Sohrab, S. H., *Combust. Flame* **64**, 193-201 (1986).
- [42] Sohrab, S. H., and Law, C. K., *Int. J. Heat Mass Transfer* **27**, 291 (1984).
- [43] Chen, Z. H., Lin, T. H., and Sohrab, S. H., *Combust. Sci. Technol.* **60**, 63 (1988).
- [44] Turns, R. S., *An Introduction to Combustion*, McGraw Hill, New York, 1996, p.221.